

Space-Time Observation of Brain Activity

Brian D. Ripley

Professor of Applied Statistics
University of Oxford

`ripley@stats.ox.ac.uk`

`http://www.stats.ox.ac.uk/~ripley/talks.html`

Outline

Joint work with Jonathan Marchini (as a D.Phil student).

Part 1: Magnetic Resonance Imaging of Brain Structure

Data, background and advice provided by Peter Styles (MRC Biochemical and Clinical Magnetic Resonance Spectroscopy Unit, Oxford)

Part 2: Statistical Analysis of Functional MRI Data

Data, background and advice provided by Stephen Smith (Oxford Centre for Functional Magnetic Resonance Imaging of the Brain) and Nick Lange (McLean Hospital, Harvard).

Magnetic Resonance Imaging



Magnetic resonance imaging is a non-invasive way of examining a living brain as it functions. We will only consider human brains, but work is also done on rat brains, which are smaller and can be given more interference.

In MRI can trade temporal, spatial and spectral resolution. Data is acquired in Fourier domain over a period, down to around 3 seconds. The subject is immersed in a strong magnetic field (needs powerful magnets—that in Oxford is 3 Tesla) and responses to input signals allow information to be collected simultaneously spatially. The sorts of information are

- spin decay rates of hydrogen atoms, longitudinally and transversally (T1 and T2).
- BOLD, measurements of presence of oxygenated blood.
- perfusion of blood.
- presence of specific chemicals.

Collect one or more over ca 45 minutes in the scanner.

Data rates

A typical experiment will collect information on up to $256 \times 256 \times 30$ voxels. This could be collected at up to 200 time points, and on several quantities.

Typically one experiment yields 1–100 million observations. There are be a few hundred sessions (a few on up to 100 subjects) in the course of a medical/psychological/drug study.

Data collection is expensive, especially on research machines.

More ‘powerful’ machines are also more unreliable, and may produce less precise results than production machines unless very well tuned.

Part 1:

MRI Studies of Brain Structure

Neurological Change

Interest is in the change of tissue state and neurological function after traumatic events such as a stroke or tumour growth and removal. The aim here is to identify tissue as normal, impaired or dead, and to compare images from a patient taken over a period of several months.

In MRI can trade temporal, spatial and spectral resolution. In MR spectroscopy the aim is a more detailed chemical analysis at a fairly low spatial resolution. In principle chemical shift imaging provides a spectroscopic view at each of a limited number of voxels: in practice certain aspects of the chemical composition are concentrated on.

Pilot Study

Our initial work has been exploring 'T1' and 'T2' images (the conventional MRI measurements) to classify brain tissue automatically, with the aim of developing ideas to be applied to spectroscopic measurements at lower resolutions.

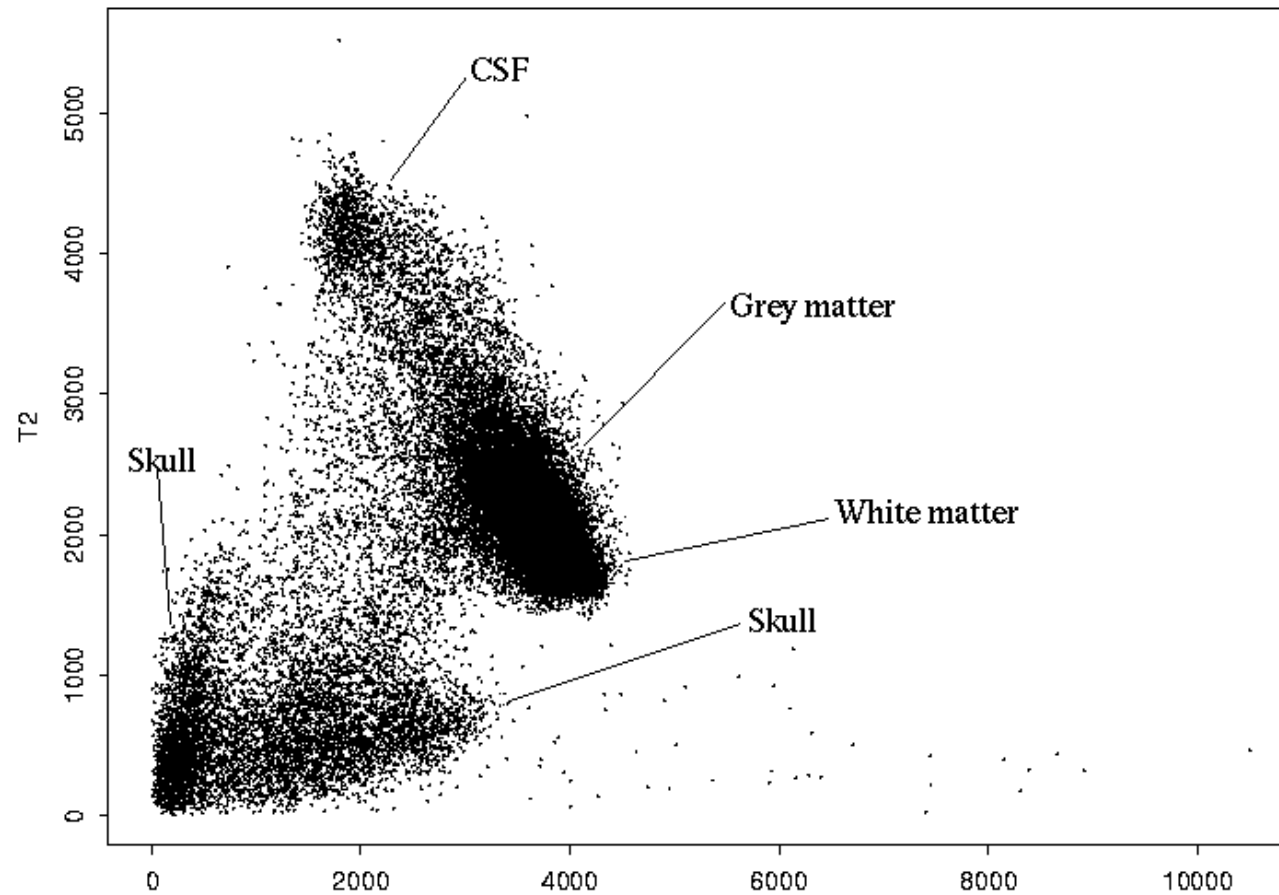
Consider image to be made up of 'white matter', 'grey matter', 'CSF' (cerebro-spinal fluid) and 'skull'.

Initial aim is reliable automatic segmentation. Since applied to a set of patients recovering from severe head injuries.

Some Data



T1 (left) and T2 (right) MRI sections of a 'normal' human brain.
This slice is of 172×208 pixels. Imaging resolution was $1 \times 1 \times 5$ mm.



Data from the same image in T1–T2 space.

Imaging Imperfections

The clusters in the T1–T2 plot were surprising diffuse. Known imperfections were:

- (a) ‘Mixed voxel’ / ‘partial volume’ effects. The tissue within a voxel may not be all of one class.
- (b) A ‘bias field’ in which the mean intensity from a tissue type varies across the image. This effect is thought to vary approximately multiplicatively and to consist of a radial component plus a linear component, the latter varying from day to day.
- (c) The ‘point spread function’. Because of bandwidth limitations in the Fourier domain in which the image is acquired, the true observed image is convolved with a spatial point spread function of ‘sinc’ ($\sin x/x$) form. The effect can sometimes be seen at sharp interfaces (most often the skull / tissue interface) as a rippling effect, but is thought to be small.

Bias Fields

There is an extensive literature on bias field correction. One approach uses a stochastic process prior for the bias field, and is thus another re-invention of the ideas known as *kriging* in the geostatistical literature. Based on experience with the difficulty of choosing the degree of smoothing and the lack of resistance to outliers (kriging is based on assumptions of Gaussian processes) we prefer methods with more statistical content and control.

Our basic model is

$$\log Y_{ij} = \mu + \beta_{\text{class}(ij)} + s(i, j) + \epsilon_{ij}$$

for the intensity at voxel (i, j) , studied independently for each of the T1 and T2 responses. Here $s(x, y)$ is a spatially smooth function.

Of course, the equation depends on the classification, which will itself depend on the predicted bias field. This circularity is solved by iterative procedure, starting with no bias field.

Estimation

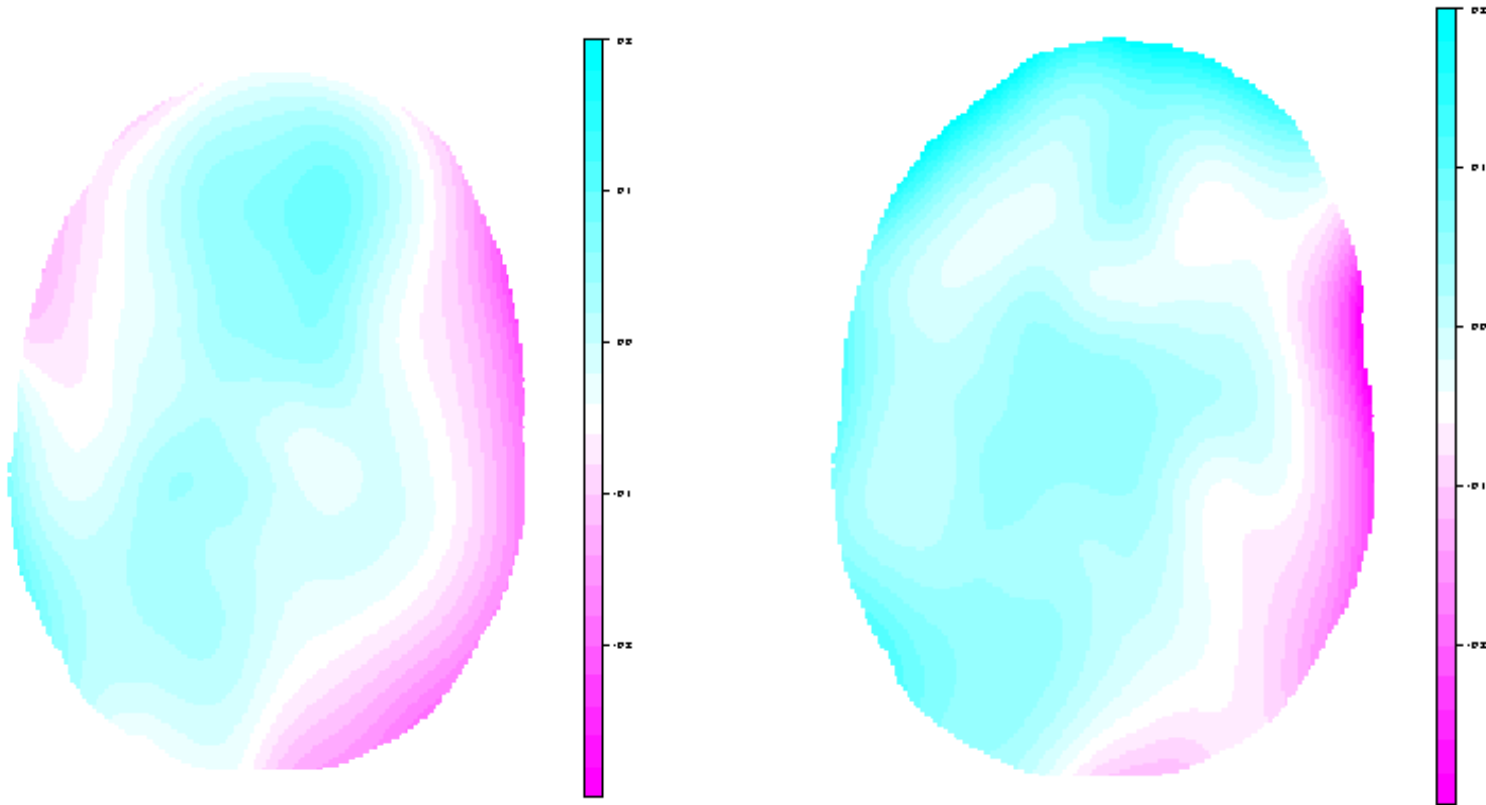
If the classification were known we would use a robust method that fits a long-tailed distribution for ϵ_{ij} , unconstrained terms α_j for each class, and a ‘smooth’ function s . We cope with unknown class in two ways. In the early stages of the process we only include data points whose classification is nearly certain, and later we use

$$\log Y_{ij} = \mu + \sum_{\text{class } c} \beta_c p(c | Y_{ij}) + s(i, j) + \epsilon_{ij}$$

that is, we average the class term over the posterior probabilities for the current classification.

For the smooth term s we initially fitted a linear trend plus a spline model in the distance from the central axis of the magnet, but this did not work well, so we switched to *loess*. Loess is based on fitting a linear surface locally plus approximation techniques to avoid doing for the order of 27 000 fits.

Fits of bias fields



Fitted ‘bias fields’ for T1 (left) and T2 (right) images.

The bias fields for these images are not large and change intensity by 5–10%.

Modelling the data

Each data point (representing a pixel) consists of one T1 and one T2 value

Observations come from a mixture of sources so we use a finite normal mixture model

$$f(y; \Psi) = \sum_{i=1}^g \pi_i \phi(y; \mu_i, \Sigma_i)$$

where the mixing proportions, π_i , are non-negative and sum to one and where $\phi(y; \mu_i, \Sigma_i)$ denotes the multivariate normal p.d.f with mean vector μ and covariance matrix Σ .

Don't believe what you are told: almost everything we were told about image imperfections from the physics was clearly contradicted by the data.

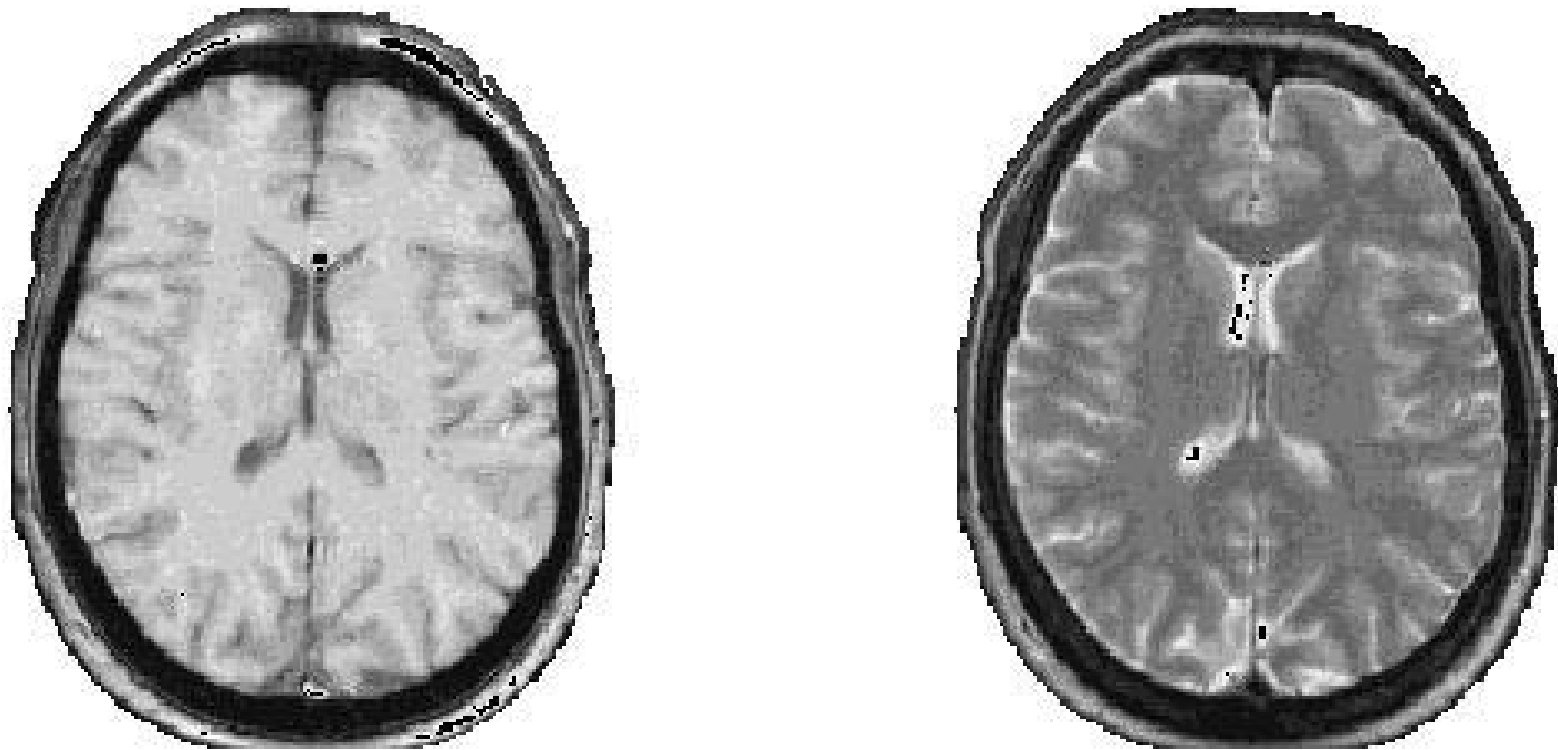
Application/Results

6 component model

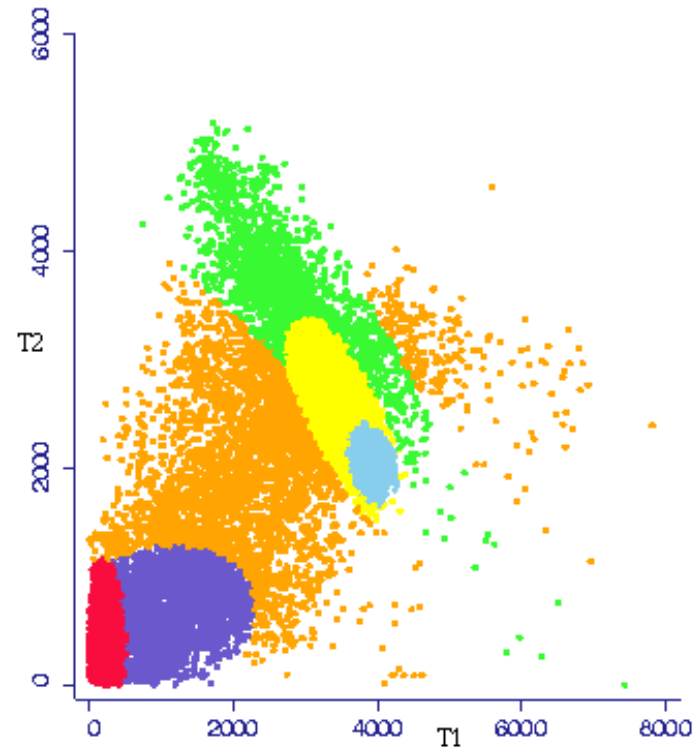
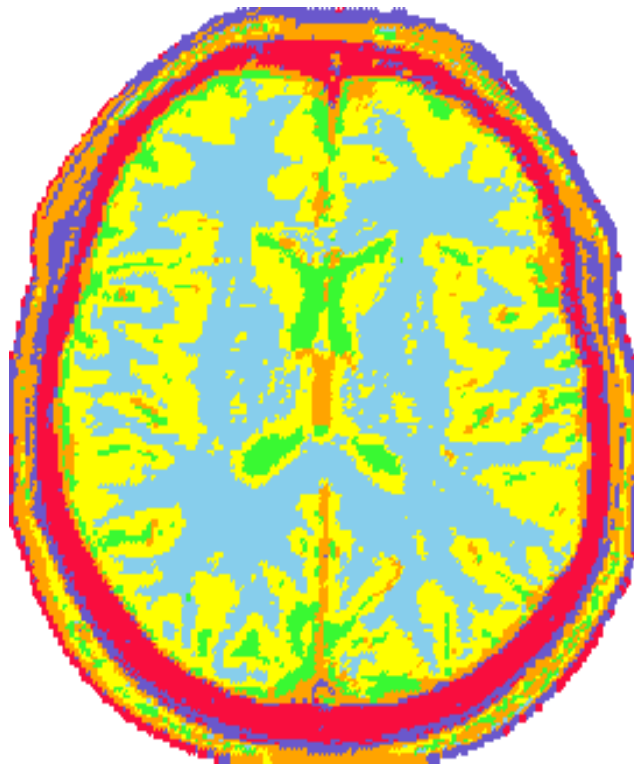
- CSF
- White matter
- Grey matter
- Skull type 1
- Skull type 2
- Outlier component (fixed mean and large variance)

Initial estimates chosen manually from one image and used in the classification of other images.

A Second Dataset



T1 (left) and T2 (right) MRI sections of another 'normal' human brain.

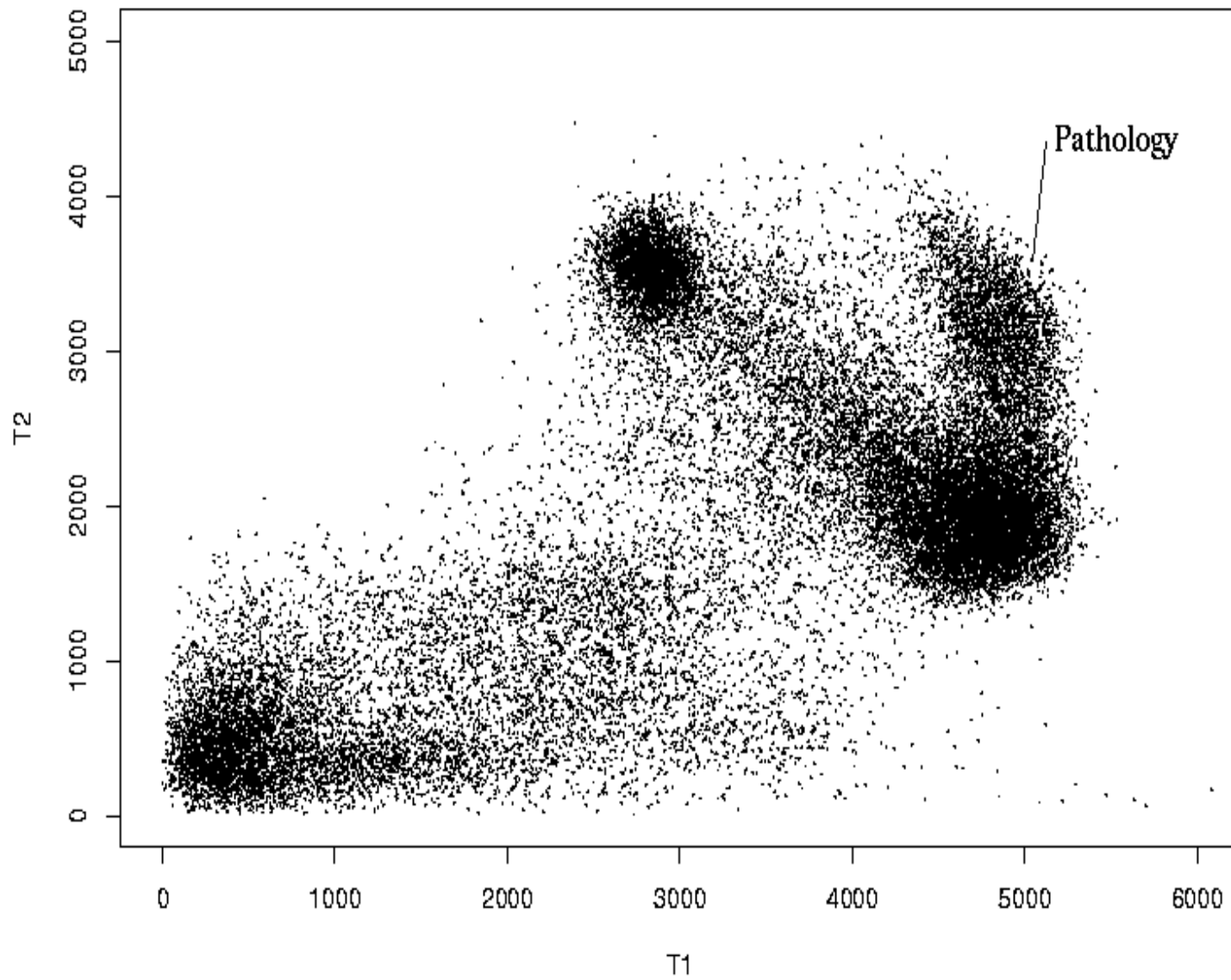


Classification image (left) and associated T1/T2 plot (right), training the 6-component mixture model from its fit on the reference subject.

Outliers and anomalies

We have found our scheme to be quite robust to variation in imaging conditions and to different ‘normal’ subjects. The ‘background’ class helps greatly in achieving this robustness as it ‘mops up’ the observations which do not agree with the model.

However, outliers can be more extreme:



T1–T2 plot of a brain slice of a brain with a pathology.

This illustrates the dangers of classifying all the points. This is a particularly common mistake when neural networks are used for classification, and we have seen MRI brain scans classified by neural networks where common sense suggested an ‘outlier’ report was the appropriate one.

The procedure presented here almost entirely ignores the spatial nature of the image. For some purposes this would be a severe criticism, as *contextual* classification would be appropriate. However, our interest in these images is not a pretty picture but is indeed in the anomalies, and for that we prefer to stay close to the raw data. The other interest is in producing summary measures that can be compared across time.

Part 2:

Statistics of Functional MRI Data

'Functional' Imaging

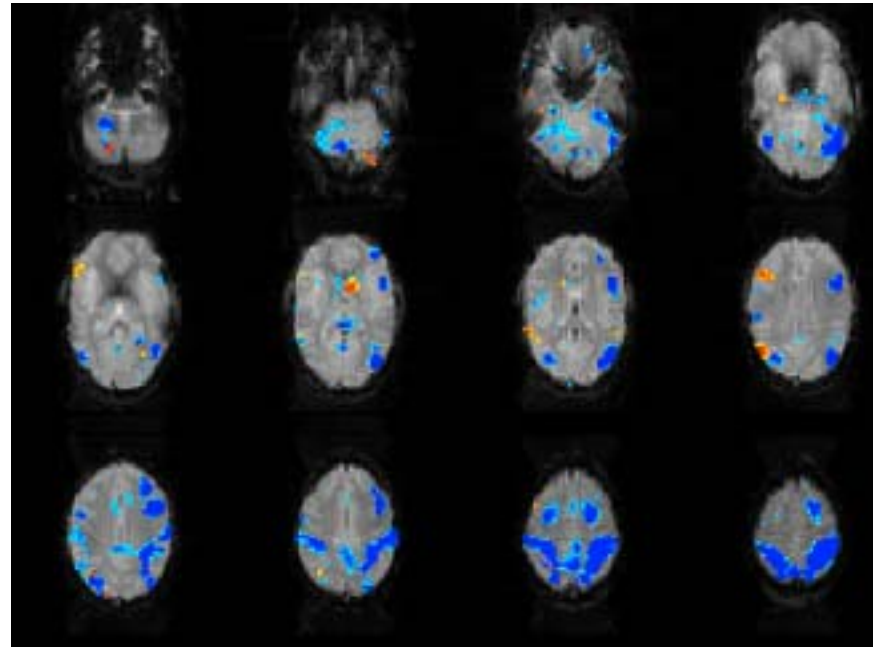
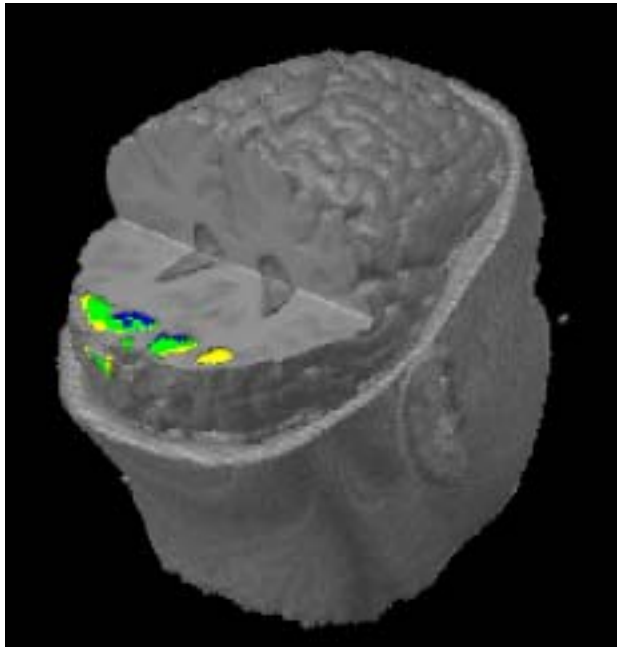
Functional PET (positron emission spectroscopy: needs a cyclotron) and MRI are used for studies of brain function: give a subject a task and see which area(s) of the brain 'light up'.

Functional studies were done with PET in the late 1980s and early 1990s, now fMRI is becoming possible. Down to $1 \times 1 \times 3$ mm voxels.

PET has lower resolution, and relies on injecting agents into the blood stream. Comparisons are made between PET images in two states (e.g. 'rest' and 'stimulus') and analysis is made on the difference image. PET images are very noisy, and results are averaged across several subjects.

fMRI has a higher spatial and temporal resolution. So most commonly stimuli are applied for a period of 10–30 secs, images taken around every 3 secs, with several repeats of the stimulus being available for one subject.

The commonly addressed statistical issue is ‘has the brain state changed’, and if so where?



Left: A pain experiment. Blue before drug administration, green after, yellow both.

Right: A verbal/spatial reasoning test, averaged over 4 subjects. 12 slices, read row-wise from bottom of head to top. Blue=spatial, red=verbal.

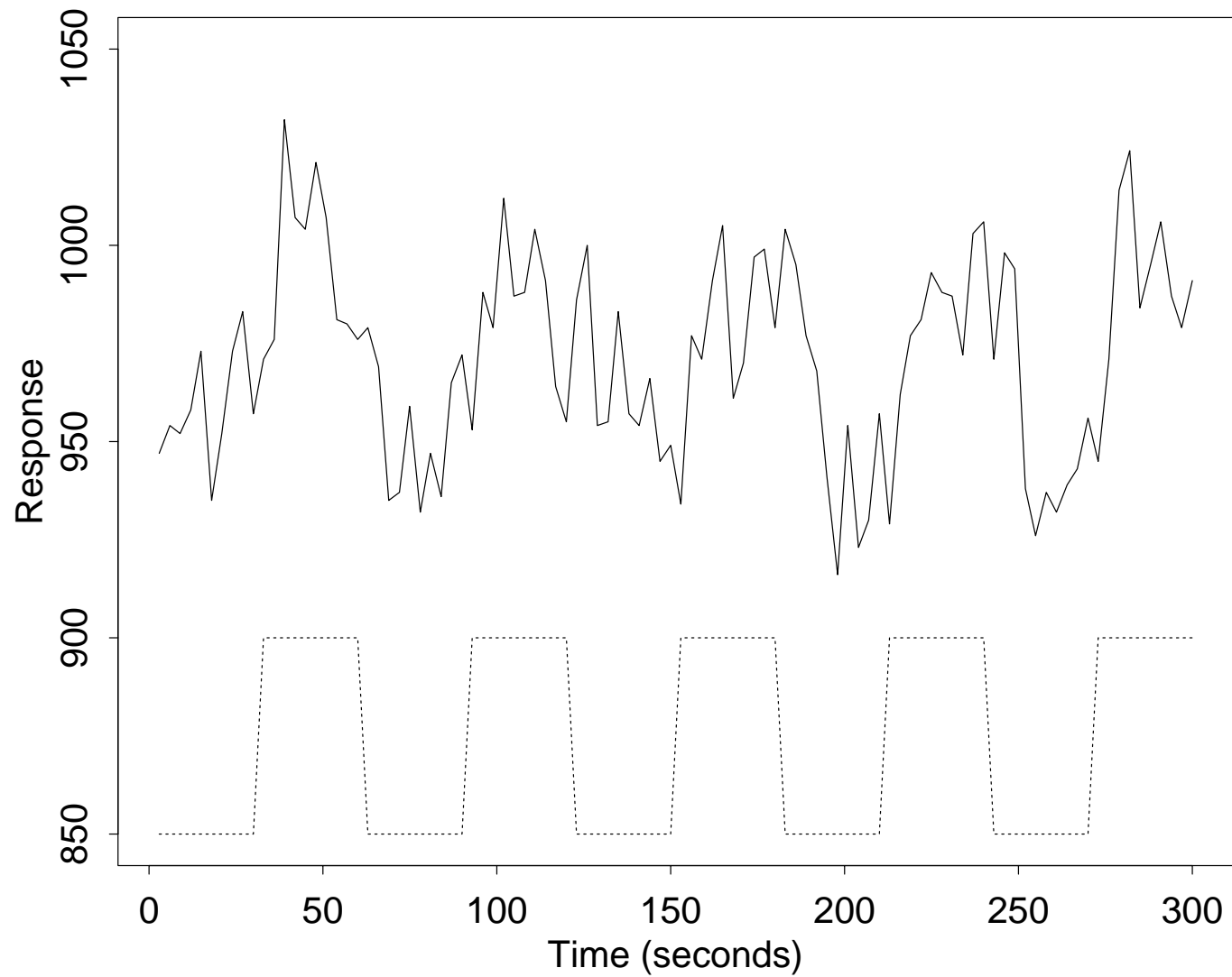
Experimental Design Issues

Some stimuli are not amenable to the 'box-car' approach. For example, pain experiments. So there are so-called single-event designs with deterministic or random intervals (to avoid subject anticipation).

What is actually observed, the BOLD effect, is both delayed and blurred by the haemodynamic response function. It is thought that the haemodynamic response occurs over 10 secs or so; this limits the temporal resolution.

Need to design these experiments much more carefully than is usual.

Perfectly possible to do more than one experiment at once, e.g. 30 secs period for visual stimulation, 45 secs period for auditory stimulation.



A real response (solid line) from a 100-scan ($TR=3\text{sec}$) dataset in an area of activation from the visual experiment. The periodic boxcar shape of the visual stimulus is shown below.

SPM

‘Statistical Parametric Mapping’ is a widely used program and methodology of Friston and co-workers, originating with PET. The idea is to map ‘ t -statistic’ images, and to set a threshold for statistical significance.

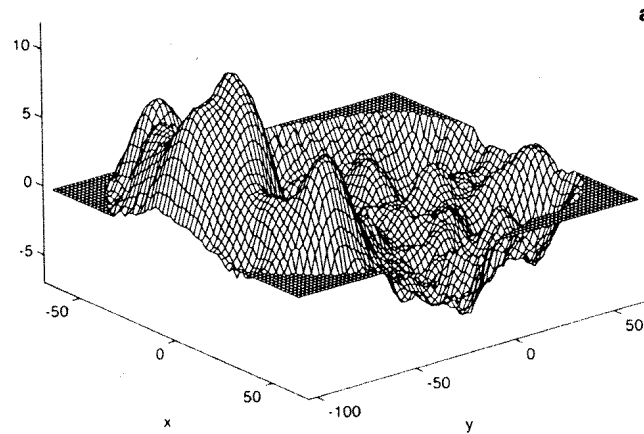
The t -statistic is in PET of a comparison between states over a number of subjects, voxel by voxel. Thus the numerator is an average over subjects of the difference in response in the two states, and the denominator is an estimate of the standard error of the numerator.

The details differ widely between studies, in particular if a pixel-by-pixel or global estimate of variance is used.

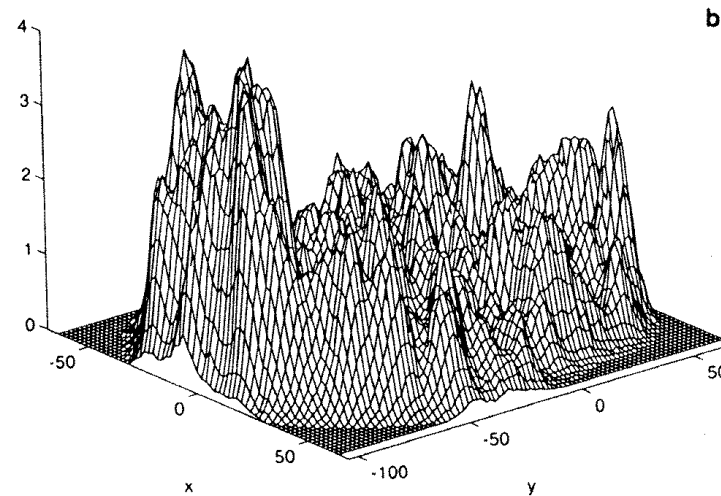
The details also vary widely between releases of and users of the programs.

Example PET Statistics Images

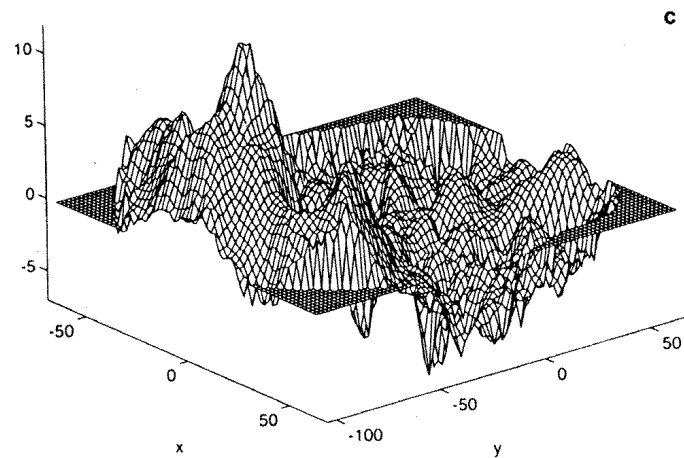
From Holmes *et al* (1996). 12 subjects, 6 A–B, 6 B–A.



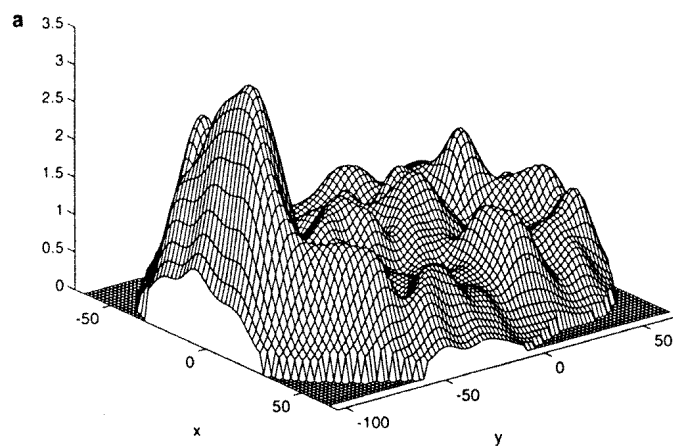
Mean difference image.



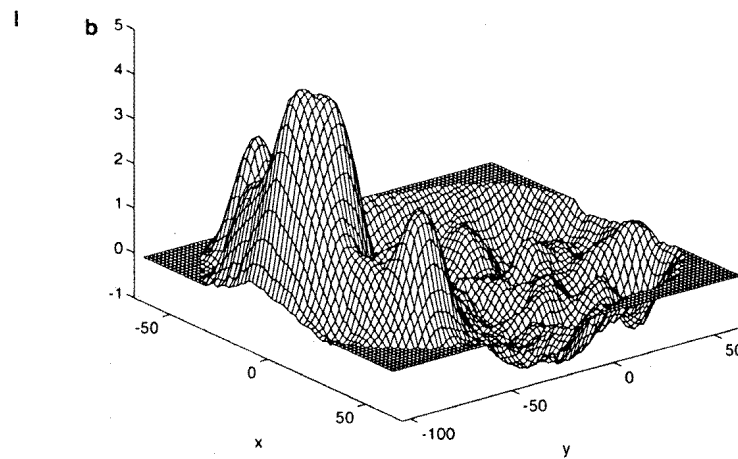
Voxel-wise variance image.



Voxel-wise t -statistic image.



Smoothed variance image.



Resulting t -statistic image.

The GLM approach

A SAS-ism: it means linear models. May take the autocorrelation of the noise (in time) into account.

- May or may not remove overall mean.
- May or may not remove trends.
- Design matrix may contain
 - An overall mean
 - A linear or other trend
 - The signal convolved with a linearly-parametrized HRF: often a couple of gammas or a gamma density and its derivative.
- The signal is usually filtered by a matrix S , so the model becomes

$$SY = SX\beta + S\epsilon, \quad \epsilon \sim N(0, \sigma^2 V(\theta))$$

Variations on the theme in a series of papers by Friston *et al*:

Analysis of functional MRI time-series

Analysis of functional MRI time-series revisited

Analysis of functional MRI time-series revisited—again

All fit β by least-squares, but differ in the estimate used of σ^2 . The third paper suggests a scaled version of the residual MSq.

Not exactly unknown statistical theory (to statisticians)!

Two main issues:

1. What is the best estimate $\hat{\beta}$ of β ?
2. What is a good (enough) estimate of its null-hypothesis variability, $\text{var}(\hat{\beta})$?

Multiple comparisons

Finding the voxel(s) with highest SPM values should detect the areas of the brain with most change, but does not say they are significant changes. The t distribution *might* apply at one voxel, but it does not apply to the voxel with the largest response.

Conventional multiple comparison methods (e.g. Bonferroni) may over-compensate if the voxel values are far from independent.

Three main approaches:

1. Randomization-based analysis (Holmes *et al*) across replications.
2. (High) level crossings of Gaussian stochastic processes (Worsley *et al*): *Euler characteristics*.
3. Variability within the time series at a voxel.

Randomization-based Statistics

Classical statistical inference of designed experiments is based on the uncertainty introduced by the randomization, and not on any natural variability.

A typical fPET or fMRI experiment compares two states, say A and B. If there is no difference between the states we can flip the labels within each pair (for each subject in PET, for each repetition \times subject in fMRI). If there are n pairs, there are 2^n possible A–B or B–A labellings. If there is no difference, these all give equally likely values of an observed statistic, so compared observed statistic to the permutation distribution.

Can choose any statistic one can compute fairly easily.

Holmes *et al.* actually used a restricted randomization, keep the balance of their 12 pairs into 6 A–B and 6 B–A pairs.

Euler Characteristics

The Worsley *et al* approach is based on modelling the SPM image X_{ijk} as a Gaussian (later relaxed) stochastic process in continuous space with a Gaussian autocorrelation function (possibly geometrically anisotropic). The autocorrelation function must be estimated from the data, but to some considerable extent is imposed by low-pass filtering.

For such processes there are results (Hasofer, Adler) on the level sets $\{\mathbf{x} : X(\mathbf{x}) > x_0\}$. These will be made up of components, themselves containing holes. The results are on the expected Euler characteristic (number of sets minus holes) as function of x_0 , but for large x_0 there is a negligible probability of a hole, and the number is approximately Poisson distributed. Thus we can choose x_0 such that under the null hypothesis

$$P(X(\mathbf{x}) > x_0 \text{ for any } \mathbf{x} \in A) \approx 5\%$$

Note that this is based on variability within a single image to address the multiple comparisons point.

Time-Series-based Statistics

The third component of variability is within the time series at each voxel. Suppose there were no difference between A and B. Then we have a stationary autocorrelated time series, and we want to estimate its mean and the standard error of that mean.

This is a well-known problem in the output analysis of (discrete-event) simulations.

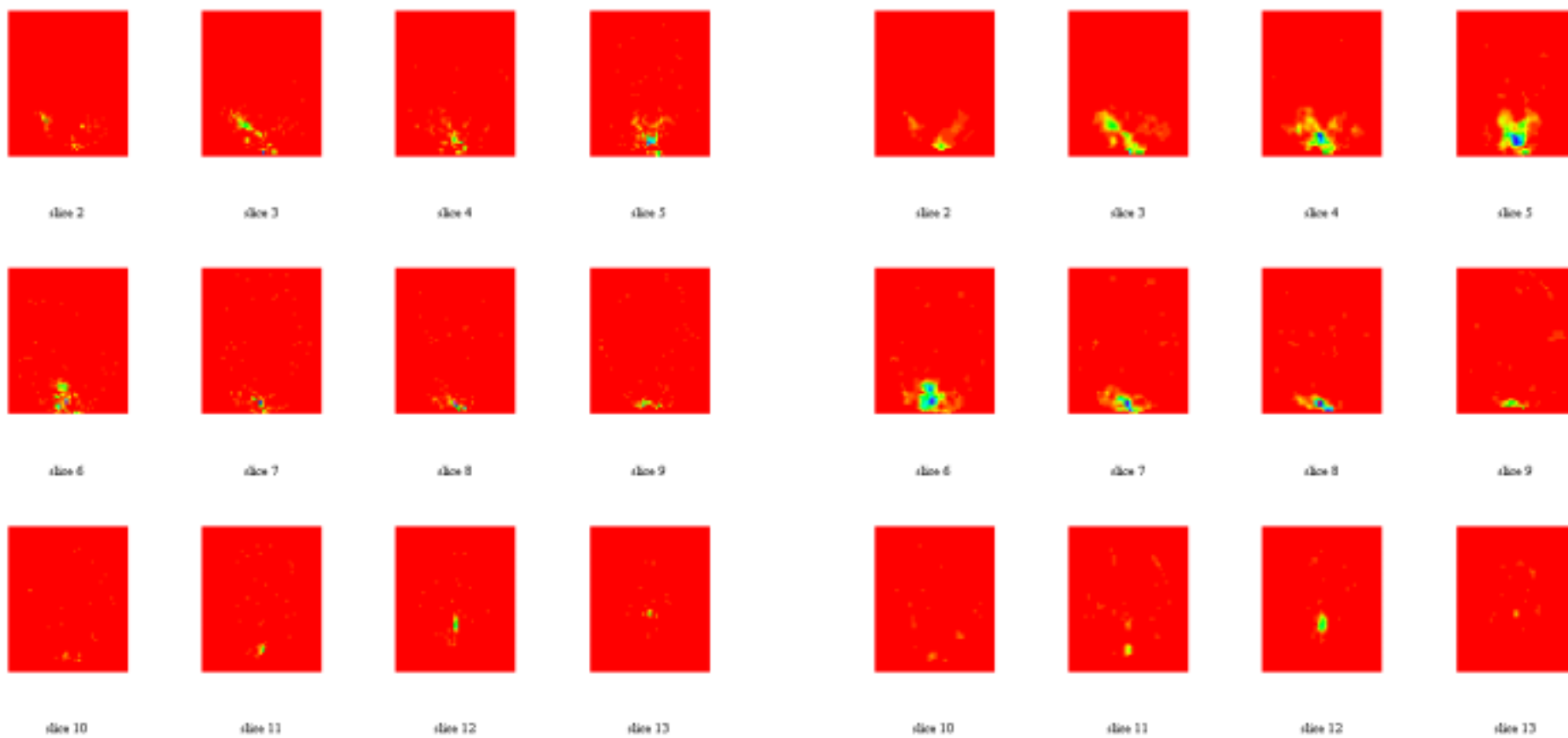
More generally, we want the mean of the A and B phases, and there will be a delayed response (approximately known) giving a cross-over effect. Instead, use a matched filter (sin wave?) to extract effect, and estimated autocorrelations (like Hannan estimation) or spectral theory to estimate variability. For a sin wave the theory is particularly easy: the log absolute value of response has a Gumbel distribution with location depending on the true activation.

fMRI Example

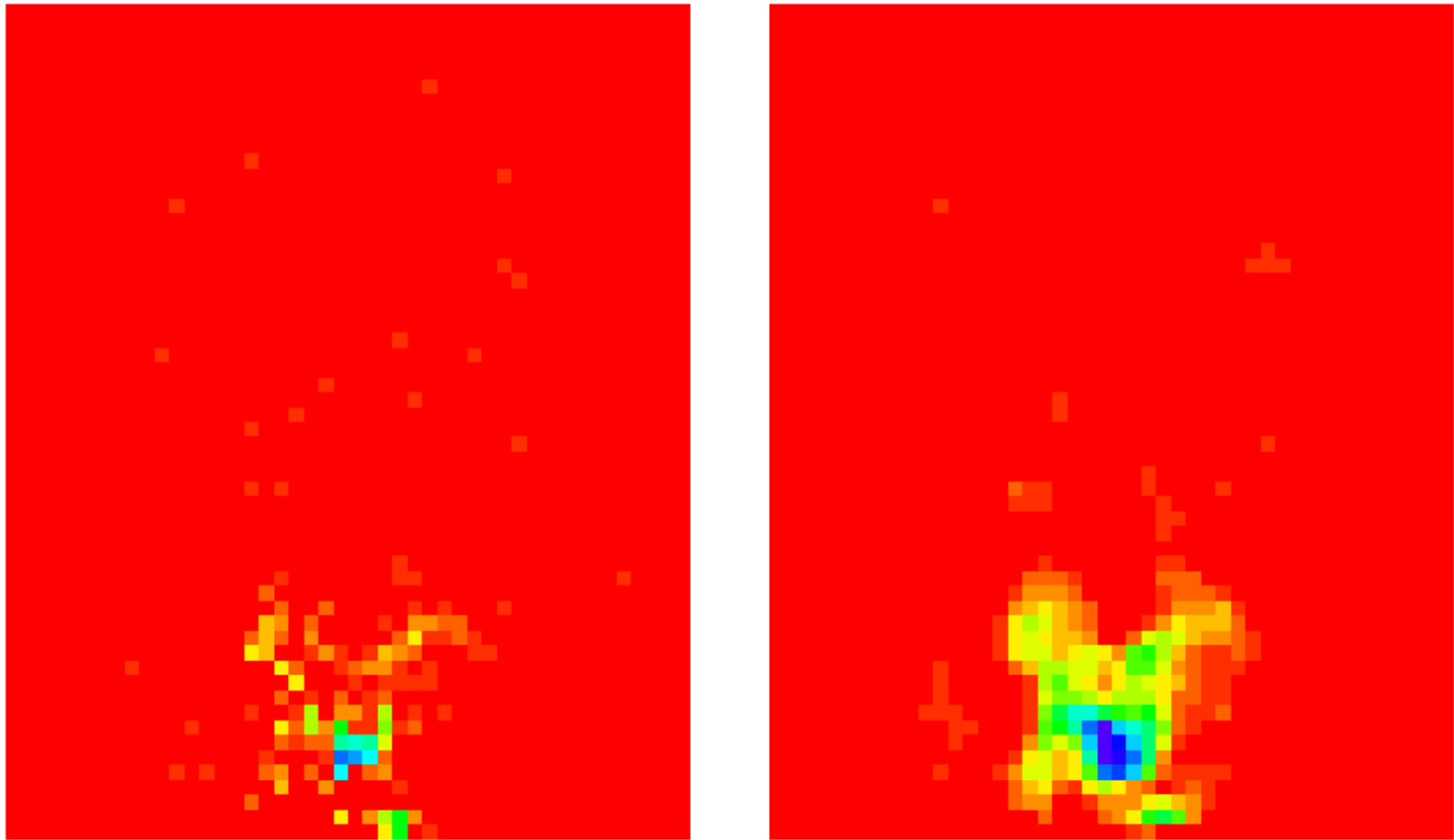
Data on $64 \times 64 \times 14$ grid of voxels. (Illustrations omit top and bottom slices and areas outside the brain, all of which show considerable activity, probably due to registration effects.)

A series of 100 images at 3 sec intervals: a visual stimulus (a striped pattern) was applied after 30 secs for 30 secs, and the A–B pattern repeated 5 times. In addition, an auditory stimulus was applied with 39 sec ‘bursts’.

Conventionally the images are filtered in both space and time, both high-pass time filtering to remove trends and low-pass spatial filtering to reduce noise (and make the Euler characteristic results valid). The resulting t -statistics images are shown on the next slide. These have variances estimated for each voxel based on the time series at that voxel.

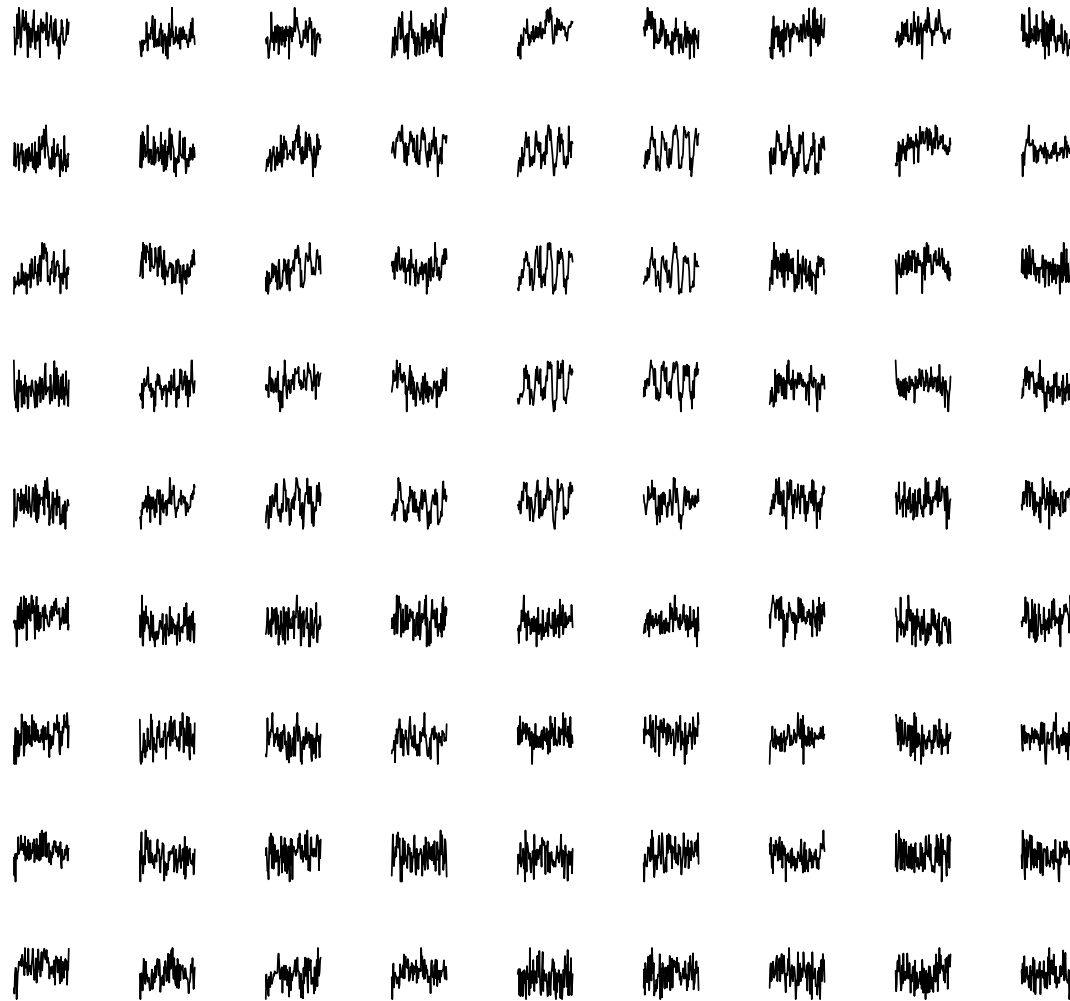


SPM99 t -statistic images, with spatial smoothing on the right



Slice 5, with spatial smoothing on the right

A Closer Look at some Data

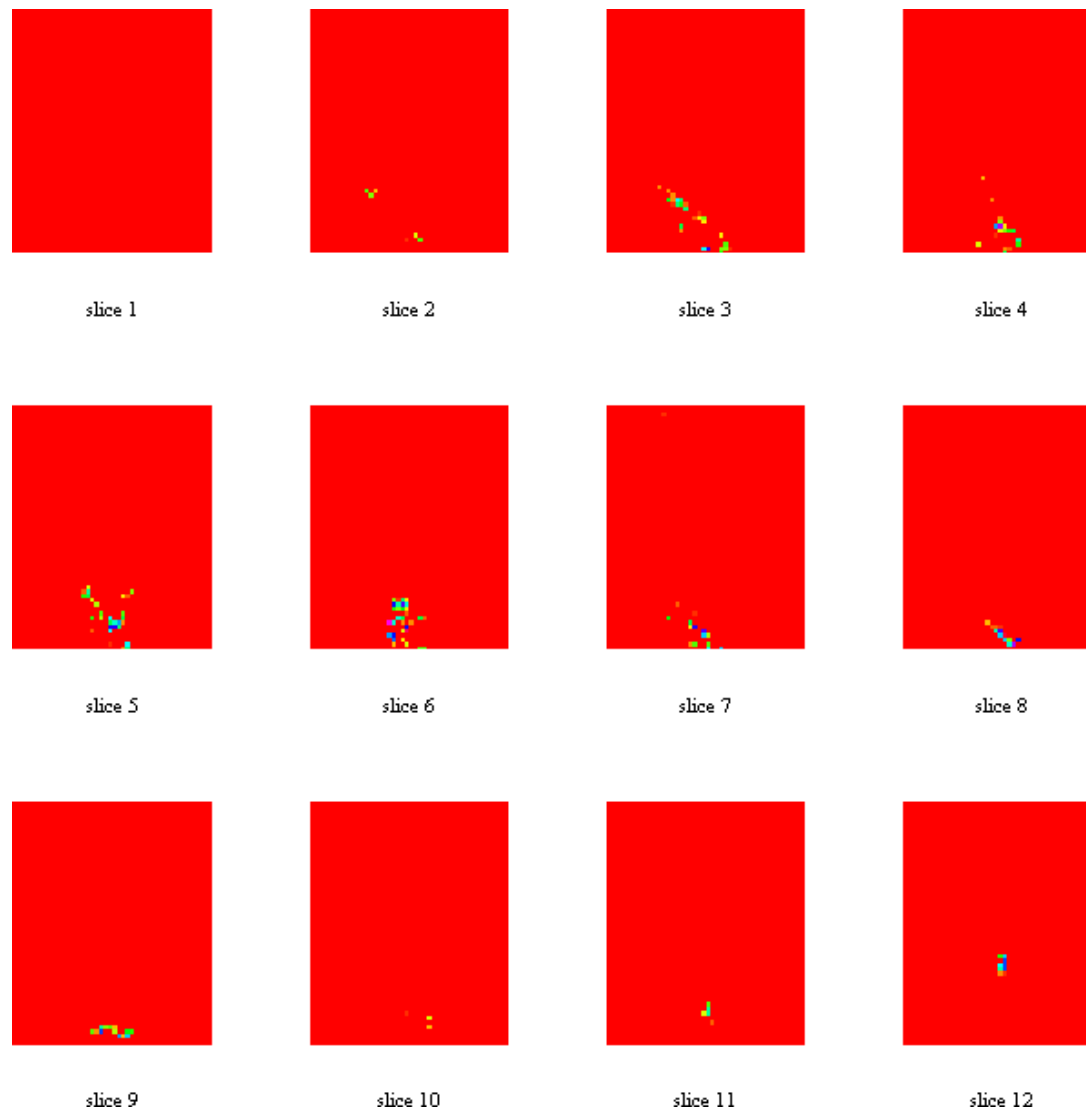


A 10×10 grid in an area of slice 5 containing activation.

Alternative Analyses

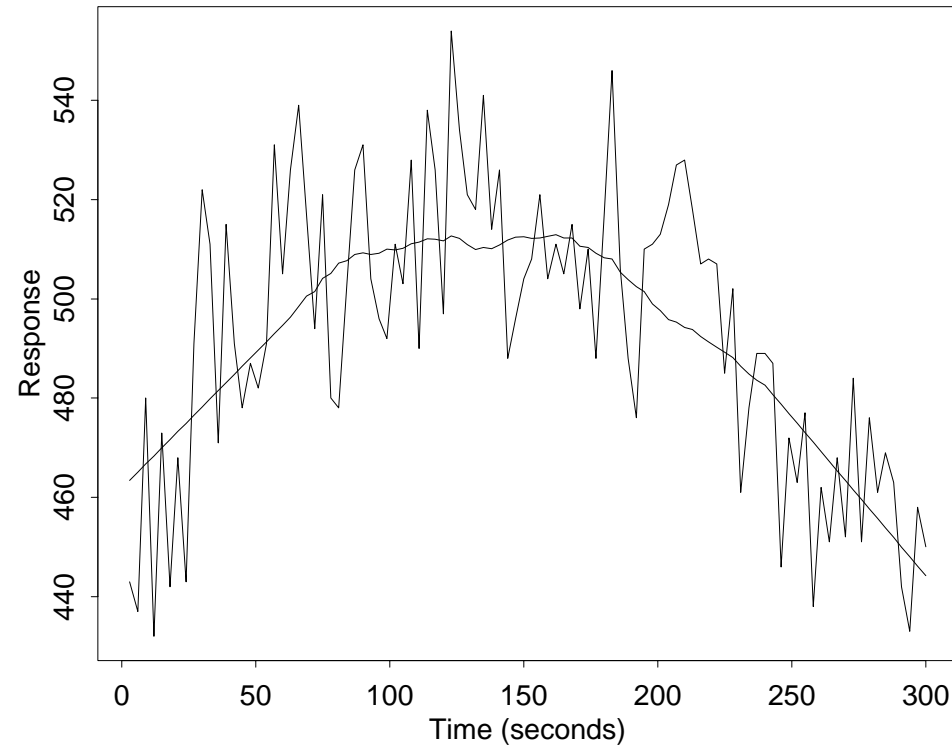
- Work with raw data.
- Non-parametric robust de-trending, Winsorizing if required.
- Work in spectral domain.
- Match a filter to the expected pattern of response (square wave input, modified by the haemodynamic response).
- Non-parametric smooth estimation of the noise spectrum at a voxel, locally smoothed across voxels.
- Response normalized by the noise variance should be Gumbel (with known parameters) on log scale.

This produced much more extreme deviations from the background variation, and much more compact areas of response. 30–100 minutes for a brain (in S / R on ca 400MHz PC).



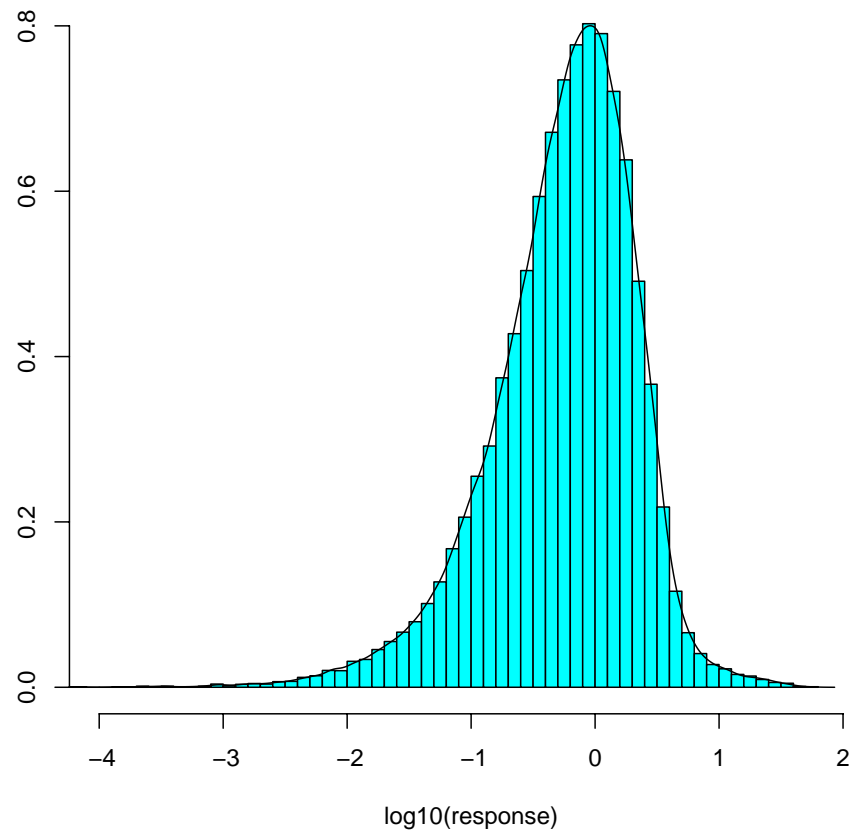
Log abs filtered response, with small values coloured as background (red). Threshold for display is $p < 10^{-5}$ (and there are ca 20,000 voxels inside the brain here).

Trend-removal



A voxel time series from the dataset showing an obvious non-linear trend.

We used a running-lines smoother rejecting outliers (and Winsorizing the results).

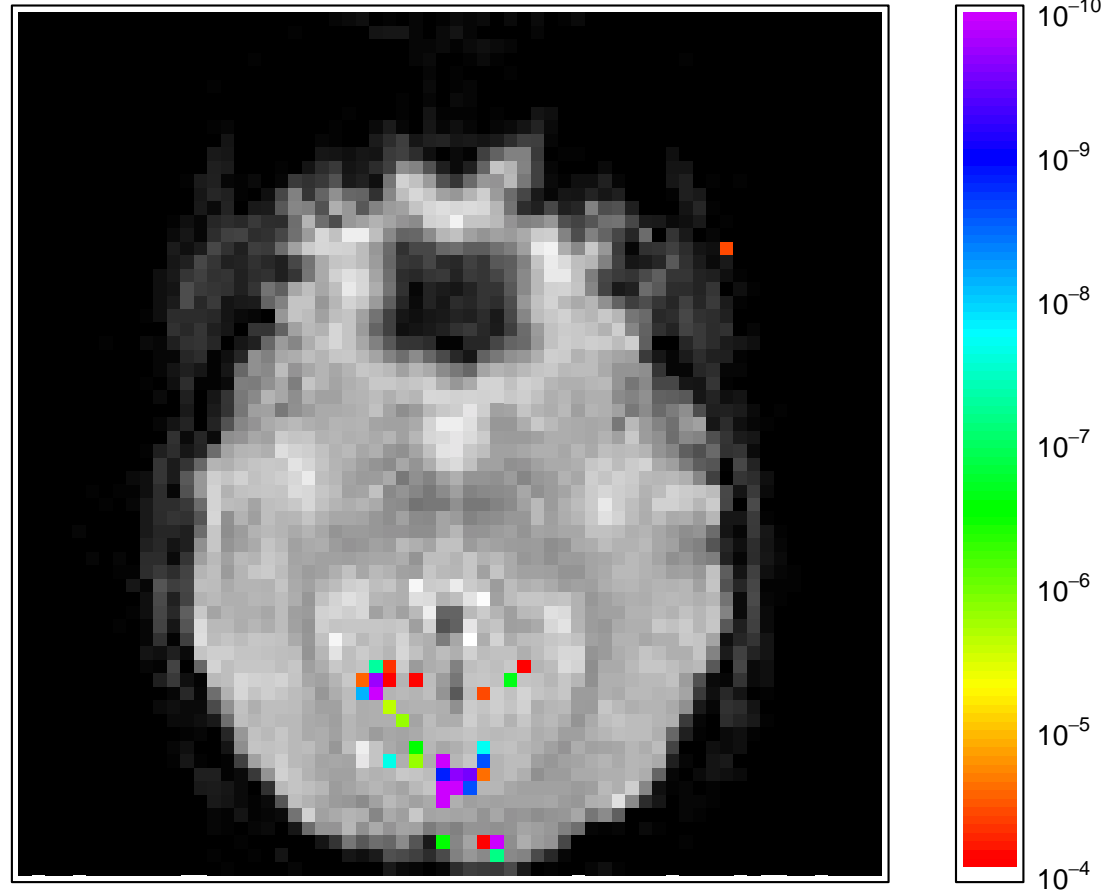


Histogram of log filtered response, for an image with activation.

We can validate the distribution theory by looking at frequencies without stimulus, and ‘null’ images.

Plotting p values

p -value image of slice 5 thresholded to show p -values below 10^{-4} and overlaid onto an image of the slice. Colours indicate differential responses within each cluster. An area of activation is shown in the visual cortex, as well as a single 'false-positive', that occurs outside of the brain.



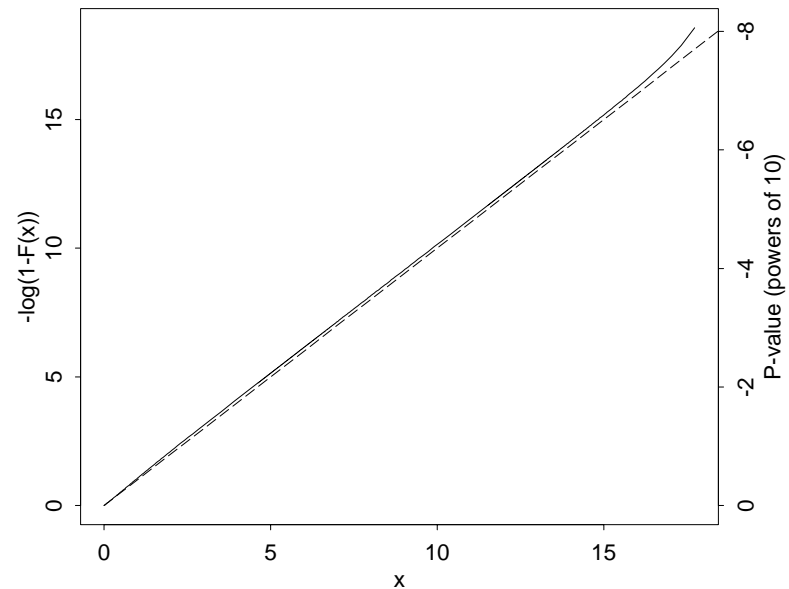
Calibration

Before we worry about multiple comparisons, are the t -statistics (nearly) t -distributed?

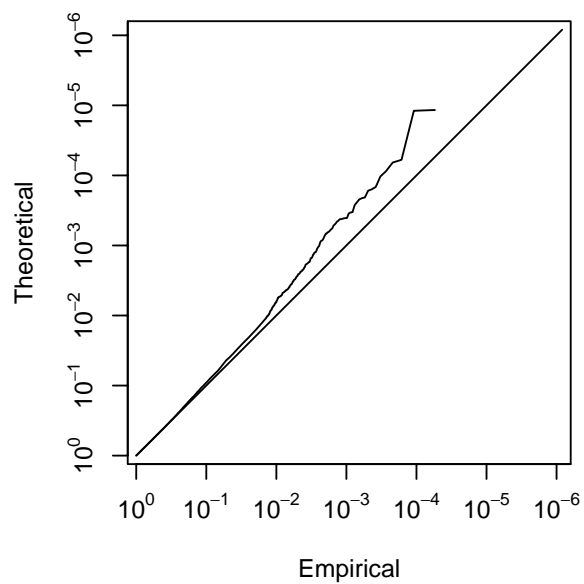
Few people have bothered to check, and those who did (Bullmore, Brammer *et al*, 1996) found they were not.

We can use null experiments as some sort of check.

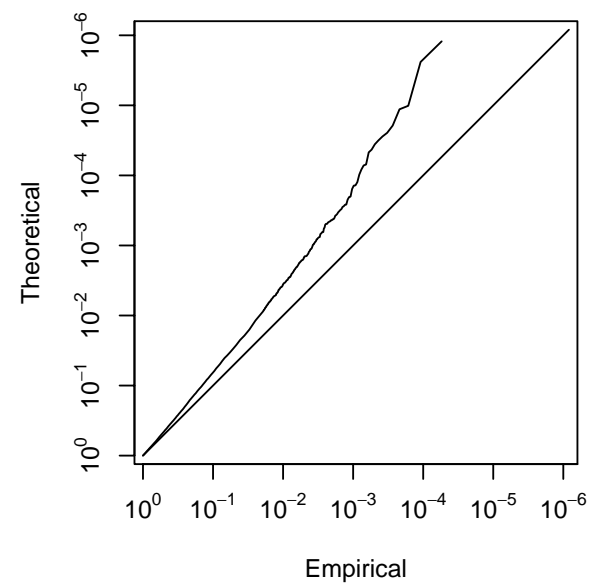
In our analysis we can use other frequencies to self-calibrate, but *we* don't need to:



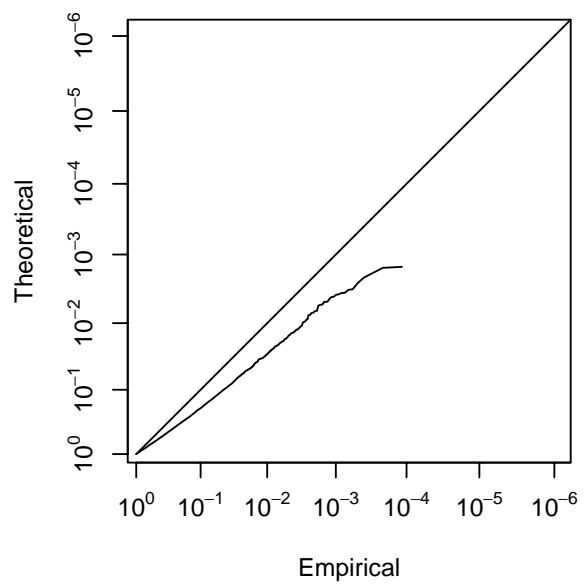
Bullmore et al.



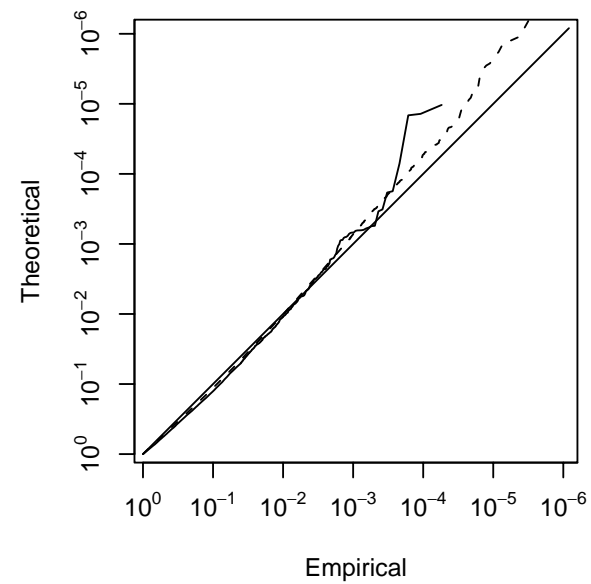
AR(1) + non-linear detrending



SPM99



This paper



Conclusions

- Look at your data (even if it is on this scale: millions of points per experiment).
- Data ‘cleaning’ is vital for routine use of such procedures.
- Fit your theory to your analysis, not *vice versa*.
- You need to be sure that the process is reliable, as no one can check on this scale.
- There is no point in building sophisticated methods on invalid foundations.
- It is amazing what can be done in high-level languages on cheap computers.